On the passband of head-parallax displays

A. Boev and R. Bregović, "On the passband of head-parallax displays," *Proc. SPIE-EI: Image Processing: Algorithms and Systems XII*, San Francisco, USA, Feb. 2014, 10 pages.

On the passband of head-parallax displays

Atanas Boev, Robert Bregovic
Department of Signal Processing, Tampere University of Technology, Tampere, Finland

ABSTRACT

We present a methodology to assess objective visual quality of multi-view and light-field displays. We consider the display as a signal processing channel and study its ability to deliver a signal while introducing negligible distortions. We start by creating a model of a display, which represents its output as a set of rays in a specific (x, y, o) coordinate space. We created a simulation framework that can use the model and render the expected output of the display for a given observation position. The framework employs an image analysis block, which aims to predict the perceptual effect of the introduced distortions and judge if the original signal is still predominant in the output. Using the framework, we can try a large set of test signals against the display model and find the ones, which are represented with sufficiently low distortion levels. We use test signals, which contain gradually changing frequency components, and use the results of the tests to build the so-called *3D passband* of the display. The 3D passband can be used as a quantitative measure of the display's ability to faithfully represent image details. The size of the passband is indicative of the spatial and angular resolution of the display.

We created two display models to serve as an example case for out framework. One model represents a typical multi-view display, and the other is representing a typical projection-based light-field display. We estimate the passband for each display model and present the results. The resulting passbands suggest, that for a given "ray-budget", the ray distribution typical for light-field displays results on a wider and more uniform passband than in the case with multi-view displays.

Keywords: autostereoscopic displays, light-field, multi-view, head-parallax, 3D displays, visual quality, signal distortions, display passband

1. INTRODUCTION

The family of displays known as *3D displays* aim to generate realistic representation of a 3D scene[1]. They achieve this by providing separate image to each eye of the observer, which allows creation of *binocular depth cues*[2]. The first generation of 3D displays requires the observer to wear special glasses, in order to separate the images intended for each eye. The second generation is the so-called *autostereoscopic displays*. Such displays can provide stereoscopic image without the need of glasses. The most common autostereoscopic displays are the *multi-view displays*[3]. They cast a set of distinctive images, known as *views*, and each image is seen from different direction. An autostereoscopic display with two views requires the observer to stay at a particular "sweet spot". Displays with larger number of views provide better angular resolution, but suffer a spatial resolution loss. The 3D displays from the third generation are able to cast a dense set of views seen from a fairly large range of observation directions. Apart from being stereoscopic, such displays can provide *head parallax* – i.e. to allow the observer to move around and see the scene from various perspectives. The third generation of displays is known as *head-parallax displays*, *quasi-holographic displays*[1] or *light-field displays*[4]. In this work we will use the term *head-parallax display* as a term that covers both display types, and to denote a display, which provides continuous parallax as a function of the observation direction.

The ability of a light-field display to deliver a faithful reproduction of a 3D scene is characterized by a multitude of parameters, such as spatial resolution, angular resolution, 3D-crosstalk, etc. It is difficult for the average consumer or to directly compare two displays, or to judge whether 3D content matches a given display. In a previous work, we introduced the concept of a *display passband*, which characterizes the display as a signal-processing channel, and measures the ability of this channel to deliver signals with various frequencies, while introducing negligible distortions. We demonstrated that such passband could be used as an indicator for the objective visual quality of a multi-view 3D display. In this work, we aim to extend the passband concept towards the general case of a head-parallax display, so it can be applied to a wide range of stereoscopic, multi-view and light-field displays.

2. HEAD-PARALLAX DISPLAYS

2.1 Multi-view 3D displays

The most common approach to build a multi-view display is to use a TFT-LCD matrix, and have an additional layer in front of the display[1]. The TFT matrix emits light trough red, green and blue-colored components, known as *sub-pixels*. The layer on top acts as an optical filter that alters the intensity of each sub-pixel and makes its visibility a function of the observation angle. Two types of optical filters are most commonly used. One is know as *lenticular sheet* - an array of magnifying lenses that is designed to magnify different sub-pixels depending on the observation direction. It redirects the light of the sub-pixels towards a set of directions as shown in Figure 1a. The other type is *parallax barrier*, and it is essentially a mask, which blocks the light in certain directions as shown in Figure 1b. The difference between the two approaches is in the amount of light that is passing through – in the case of parallax barrier, part of the light is blocked by the layer, and from any given observation angle the image on the display exhibits stripes of dark pixels, as seen in Figure 2a.

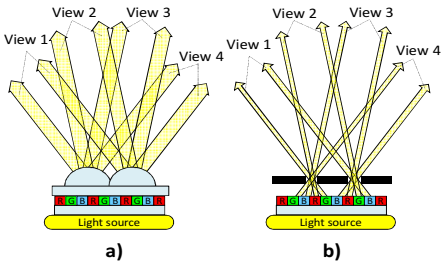

Figure 1. Optical separation in multi-view displays: a) using lenticular sheet, b) using parallax barrier

As a result of the filter for every sub-pixel there is a certain angle, from which it is perceived with maximal brightness – that angle we call *optimal observation angle* for the sub-pixel. The vector, which leaves the sub-pixel in the direction of the optimal observation angle, is the *optimal observation vector* for the sub-pixel. The optimal observation vectors for all sub-pixels of the same view are designed to intersect at a narrow spot in front of the multi-view display. From this spot, the view will be perceived with its maximal brightness. That spot is referred to as being the *optimal observation spot* of the view. As stereoscopic depth cues are perceived mostly in horizontal direction, most multi-view display designs do not allocate pixels for extra views in vertical direction[3]. The impact of the layer on the brightness of the underlying sub-pixels can be modeled as *visibility* - the ratio between the relative brightness of a view and the maximum brightness of the display as seen from the same angle. For a given observation direction, the visibility values of different sub-pixel vary in the range between 0 (not visible) and 1(fully visible). Example visibility values as measured for an 8-view multi-view display can be seen in Figure 2a [5]. The visibility of each view is as a function of the observation angle, which has peak at the optimal observation angle, and lower values for the neighboring observation points. The range of observation directions for which a view is still visible is called the *visibility zone* of a view. In order to ensure smooth transition between the neighboring views, their visibility zones overlap, and at any observation directions a few views are simultaneously visible, as seen in Figure 2b.

	Column 1			Column 2			Column 3	
row	1R	1G	1B	2R	2G	2B	3R	3G
1	0.1	0.13	0.45	0.74	0.55	0.14	0.1	0.1
2	0.11	0.25	0.73	0.66	0.19	0.11	0.1	0.09
3	0.16	0.65	0.71	0.34	0.12	0.1	0.1	0.1
4	0.45	0.74	0.55	0.14	0.1	0.1	0.1	0.13
5	0.73	0.66	0.19	0.11	0.1	0.09	0.11	0.25
6	0.71	0.34	0.12	0.1	0.1	0.1	0.16	0.65
7	0.55	0.14	0.1	0.1	0.1	0.13	0.45	0.74
8	0.19	0.11	0.1	0.09	0.11	0.25	0.73	0.66
9	0.12	0.1	0.1	0.1	0.16	0.65	0.71	0.34
10	0.1	0.1	0.1	0.13	0.45	0.74	0.55	0.14
11	0.1	0.09	0.11	0.25	0.73	0.66	0.19	0.11
12	0.1	0.1	0.16	0.65	0.71	0.34	0.12	0.1

a)

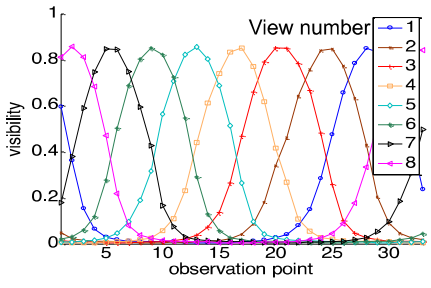

b)

Figure 2. Angular visibility of multi-view display elements: a) visibility values for neighboring pixels as seen from the same observation direction, b) angular visibility functions of different views across the observation directions

Multi-view displays have two characteristic features. The first is *spatial-multiplexing* – only part of the TFT sub-pixels is visible from a given observation direction. The second is the grouping of the sub-pixels into views – there are distinctive groups of sub-pixels, which have identical visibility function and share the same optimal observation spot. Multi-view displays that generate a large number of views can provide limited head parallax.

2.2 Projection-based light-field 3D displays

The so-called light-field displays aim to provide a continuous head parallax over a wide range of observation directions. They do so by generating a large set of light rays that originate at the screen surface and travel in various directions. One approach uses a set of digital image projectors and a special screen surface, as shown in Figure 3. Technologically, this two-stage process (scene representation and scene reconstruction) can be implemented by using an array of projection modules emitting light rays toward a custom-made light-field reconstruction surface (screen). The latter makes the optical transformation that composes rays into a continuous light-field [4]. The LF display can generate a set of rays, which travel in multiple directions, as if they were emitted from points of 3D objects at fixed spatial locations. This gives the illusion of points appearing either behind the screen, on the screen, or floating in front of it, as illustrated in Figure 3. In general, this requires a departure from the 'discrete view' formalism. Instead, a certain continuous reconstruction of the light-field emanated or reflected from the 3D visual scene is targeted. Correspondingly, the scene is represented by a discrete set of light rays, which serve as generators for the subsequent process of continuous light-field reconstruction. This technology can generate an infinite amount of rays by adding more ray generators, and can be used to create images with both horizontal and vertical parallax. For most visualization setups, horizontal parallax is sufficient to create stereoscopic and parallax depth cues. For practical reasons, light-field displays provide horizontal parallax only.

The main feature of light-field displays is the lack of discrete pixels. The set of rays visible from a given observation direction do not cross the display surface at coordinates on a rectangular grid. Additionally, light-field displays lack discrete set of views with distinctive optimal observation spots. Instead, the optimal observation vectors of each ray are evenly distributed across the whole observation range.

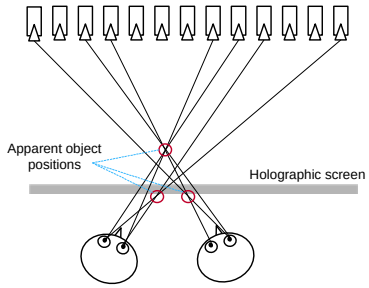

Figure 3. Light-field display architecture. Adapted from [4]

3. MODELLING OF 3D DISPLAYS

3.1 Ray-based scene representation

One way to represent a 3D scene is to describe the amount of light passing through each point in 3D space by a continuous 7-dimensional function, also known as *plenoptic function*. The function is given by $P(\theta, \varphi, \lambda, t, V_x, V_y, V_z)$, where (V_x, V_y, V_z) describe a location in the 3D space, (θ, ϑ) describe angles (directions) of observation, λ is wavelength, and t is time. An example for a ray of light described with these 7 parameters is shown in Figure 4a. As the plenoptic function is a high dimensional continuous function, it is not practical due to the large amount of data it requires. Head-parallax displays provide limited observation angles, and can show only scenes where the radiance along any ray is constant. Consequently for multi-view and light-field 3D displays, the 7-dimensional plenoptic functions can be replaced by a 4-dimensional function, also known as *two-plane representation*. The two-plane representation describes a set of rays $L(u, v, s, t)$ between two parallel planes, where the orientation of each ray is determined by the coordinates (u, v) and (s, t) where the ray is crossing each plane. An example of such representation is given in Figure 4b. Finally, for displays that provide horizontal parallax only, one can use a 3-dimensional function $L(x, y, o)$, where each vector is described by crossing a point (x, y) on a plane and a point (o) on a line. The plane is the plane of the display surface, and the line is the so-called *observation line* – a horizontal line, parallel to the display surface, as shown in Figure 4c.

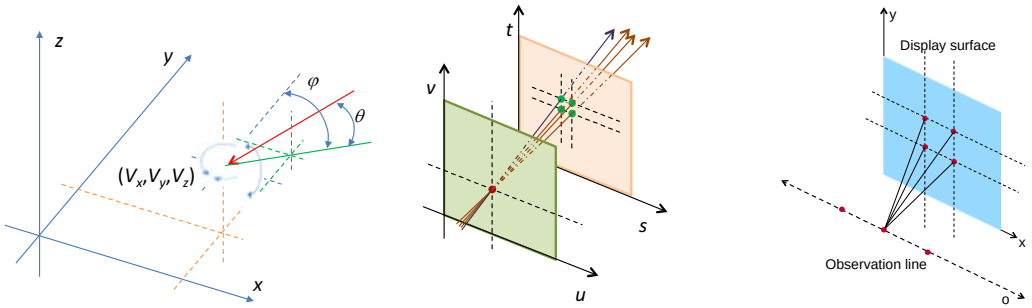

a) b) c)

Figure 4. Ray based scene representations: a) 7D plenoptic function, b) two-plane representation, c) 3D line-plane representation

In this work, we use the 3-dimensional (x, y, o) space to describe the output of a light-field display. It can be used to represent the image on the display as seen from a set of virtual cameras on the observation line, as shown in Figure 5a. The (x, y) coordinates represent points on the display surface as absolute distances from the corner of the display frame. The third coordinate, (o) represents the observation direction as absolute distance along the observation line. The point o=0 appears where the orthogonal vector leaving the center of the display crosses the observation line. Planes with different (o) coordinates represent images on the display as seen from different directions, as exemplified in Figure 5b.

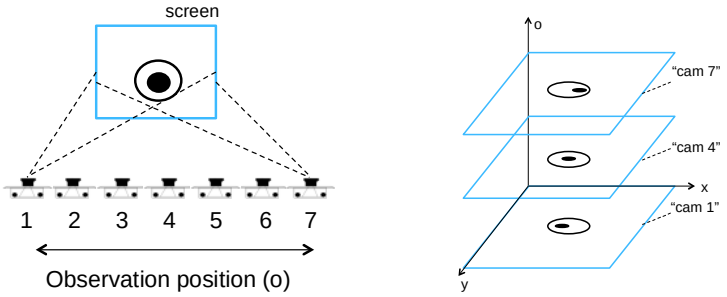

a) b)

Figure 5. 3-dimensional ray description in (x, y, o) space: a) Multiple observations of the screen from different positions along the observation line, b) the same observations "stacked-up" in continuous (x, y, o) space

3.2 Ray-based models of 3D displays

We created two display models - one to represent a multi-view display and another to represent a light-field display. Each model is represented as a set of points in (x, y, o) space, where each point describes one ray that can be generated by the display. A subset of the points, used to model of a multi-view display is shown in Figure 6. The model assumes a display size of 20cm x 20cm, and observation line of 20cm being positioned 50 cm away from the display. The (x, y) coordinates of the points appear on a grid of 512x512, which represents a TFT matrix of 512x512 pixels. The points of the grid appear on 8 different (o) coordinates, which represents a multi-view display with 8 views. Each group of points represents the sub-pixels that belong to one of the views, and are optimally visible from observation position (o). There are no two points with the same (x, y) coordinate that are optimally visible from more than one (o) position. A subset of the points from a light-field display model is shown in Figure 7. The model assumes a display size of 20cm x 20cm, and observation line of 20cm being positioned 50 cm away from the display. The (x, y) coordinates of the points in that set appear on a grid of 181x181. However, as the point sources of light-field displays do not appear on an equidistant grid, the (x, y) position of each point is randomized by adding a value in the range $\frac{20}{181}/2$ - i.e. the maximum displacement of each point from the regular grid is equal to half of the step of the grid. The optimal observation positions of each point appear in 8 sections. However, since a light-field display does not have a distinctive set of views, the (o) coordinates have been randomly distributed in each section. At each observation position there is approximately the same number of

observation points, and as the observation position (o) increases, random set of points disappear, and random set of points appear into view. Both display models use approximately the same amount of rays – the "multi-view set" has 262144 and the "light-field set" has 262088 points – a 0.02% difference.

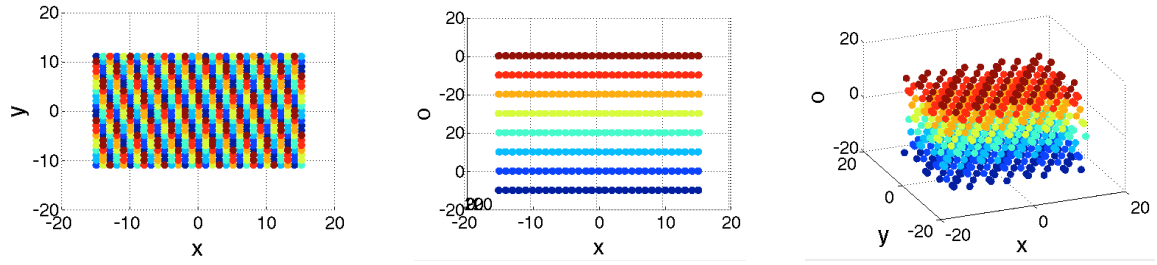

Figure 6. Set of rays modeling a multi-view display: a) x versus y plot, b) x versus o plot, c) 3D scatterplot of the set

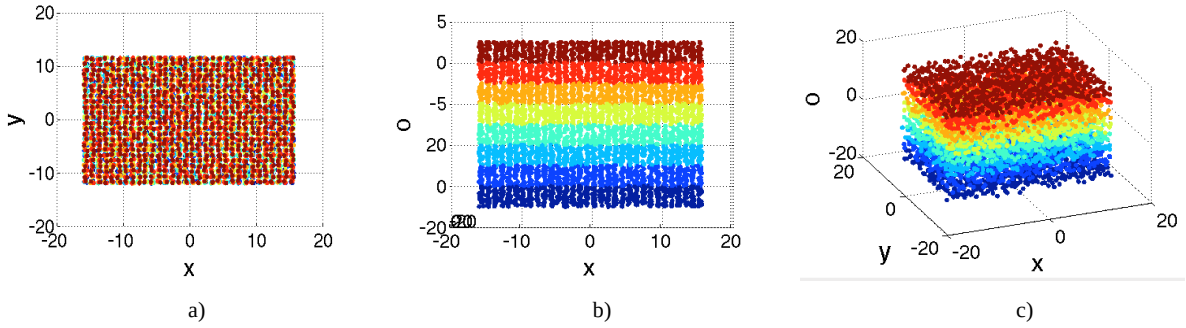

Figure 7. Set of rays, modeling a light-field display: a) x versus y plot, b) x versus o plot, c) 3D scatterplot of the set

3.3 Rendering of an arbitrary viewpoint

We have built a simulation framework, which can simulate the appearance of a test signal on a light-field display, and render the image on the display, as it would be seen from an arbitrary position on the observation line. This is done in four steps, as shown in Figure 8. The test signal is defined as a continuous function in the (x, y, o) space and a model in the same space describes the display. The first step is to sample the test signal at the (x, y, o) points which exists in the display model. Then, the angular visibility function of each ray is applied. That function "spreads" the visibility of each ray to a range of observation directions, and acts as a weighted average filter along (o) direction. For visibility weights we used the results from previous measurements of a multi-view display [5]. The angular visibility function is shown in Figure 9a. The output image for a given observation direction (o) is a plane in the (x, y, o) space. For each point in the model, we calculate the distance between the point and the plane, and project all points onto the plane. Weight for each point is calculated using the distance and the angular visibility function. This procedure "blurs" the points, stretching them in (o) direction, as shown in Figures 9b (for the multi-view model) and 9c (for the light-field model). Then, to each projected point we apply the point-spread function of a pixel, which defines the height and width of the pixel, as well as the effect of any optical diffusor in front of the pixels. Finally, the plane with elevation (o) is sampled on an equidistant grid and an output bitmap image is produced. Example images produced by the framework are shown in Figure 10. Figure 10a shows the simulation of a uniformly white image as seen on a multi-view display from the optimal observation position of one of the views. Figure 10b shows the same image as seen on the same display, but from an observation point between the optimal points for two neighboring views. Figures 10c and 10d show the simulated uniformly white image for a light-field display. The intensity fluctuation of that image is a consequence of the randomized and partially overlapping rays, after being transformed by the optical diffusor of the screen. The image is comparable to the real output of a back-projected light-field display.

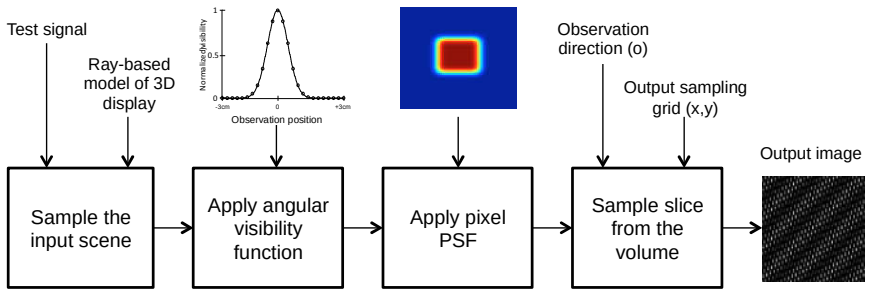

Figure 8. Block diagram of the framework, which simulates the display image as seen from an arbitrary position on the observation line

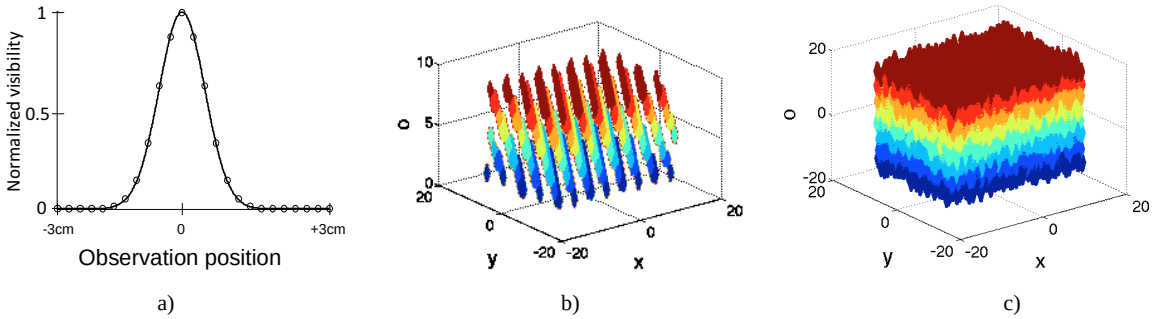

Figure 9. Angular visibility function: a) weighting coefficients as a function of the (o) distance, b) multi-view display with the weighting coefficients applied, c) light-field display model with the weighting coefficients applied.

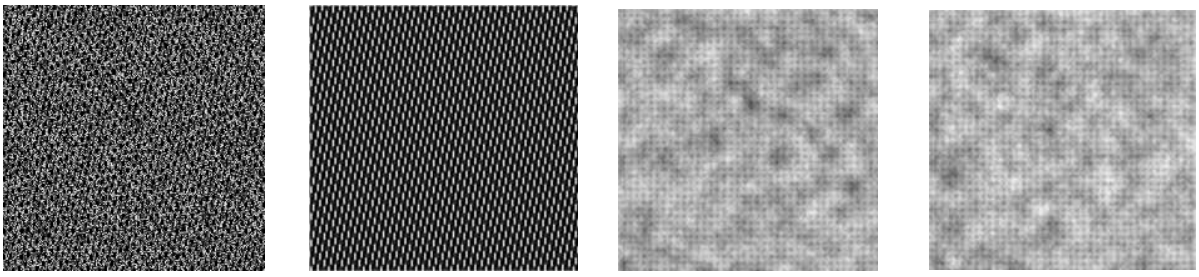

Figure 10. Example outputs of the simulation framework, simulated output for a uniformly white image: a) for a multi-view display and for o=0, b) for a multi-view display and for o=1.75cm, c) light-field display and o=0, d) light-field display and o=1.75cm

4. PASSBAND OF LIGHT-FIELD DISPLAYS

4.1 Passband evaluation methodology

In this article, we propose a methodology to evaluate the levels of distortion introduced by a light-field display. Multi-view displays suffer from masking distortions and fixed pattern noise, caused by image being produced by a set of pixels on an irregular grid. Projection based light-field displays suffer from similar problems, as the set of rays used to reconstruct the light-field are irregularly positioned in space. In both cases horizontal, vertical and angular resolution cannot be directly expressed in terms of ray density. Additionally, the visibility of such distortions depends on some properties of the human visual system, such as contrast sensitivity function (CSF) and its ability to extract the dominant spatial frequency of an image [6] (a.k.a. *gestalt principle*) [7].

In a previous work, we proposed the *display passband* as a measurement of the display performance[8]. In essence, the idea is to consider the display as a signal processing channel and to measure the distortions, introduced by the channel. The level of such distortions depends on interaction between the spectrum of the visualized content and the display's

transfer function, and it is conveniently expressed in the frequency domain. As CSF is also expressed in terms of frequency, one needs to study the performance of the display in frequency domain. In an earlier work, we evaluated the 2D passband of the display by using a set of test images and measuring the level of introduced distortions for each case[8]. The images are sinusoidal gratings with varying orientation and density, built by rendering combinations of horizontal and vertical sinusoidal frequency. For each case, we measured the amplitude of the dominant frequency and the amplitude of the second highest peak. If the ratio between the dominant peak (intended signal) and the second peak (introduced by distortions in the channel) exceeds a certain thresholds, we deem the distortions too high, and the test signal not belonging to the passband of the display. By scanning all combinations of horizontal and vertical frequencies, and doing a pass/fail analysis for each case, we build the 2D passband of the display.

In this work, we aim to extend the concept of passband to include signals that change with the observation direction. In order to do so, we create a set of test signals with three sinusoidal components – horizontal, vertical and angular frequency. We update our pass/fail analysis to assess the perceptual impact of distortions of signals that vary with the observation direction. By trying a set of test signals against the model of a light-field display, one can derive a 3-dimensional passband of the display (for horizontal, vertical and angular components), which we call its *3D passband*.

4.2 Pass/fail analysis

The aim of the pass/fail analysis is to determine if the distorted signal bears the same visual information as the intended one. When presented with a set of overlapping spatial frequencies, the HVS is able to isolate the dominant one, and reconstruct missing details from a structure. For example, a human observer is aware that the images in Figures 11a and 11b represent the same slanted sinusoidal grating, even though there is a second grating superimposed over the first one. In our analysis, we try to estimate if the dominant frequency component in the original signal is still dominant in the distorted one. If the amplitude of the second-largest peak exceeds 25% of the amplitude of the largest one, we assume that the dominant frequency is lost[8]. If for a given test signal, the dominant frequency is masked by the distortions introduced by the display then the display cannot represent that signal properly, and the signal of that frequency does not belong to display's passband.

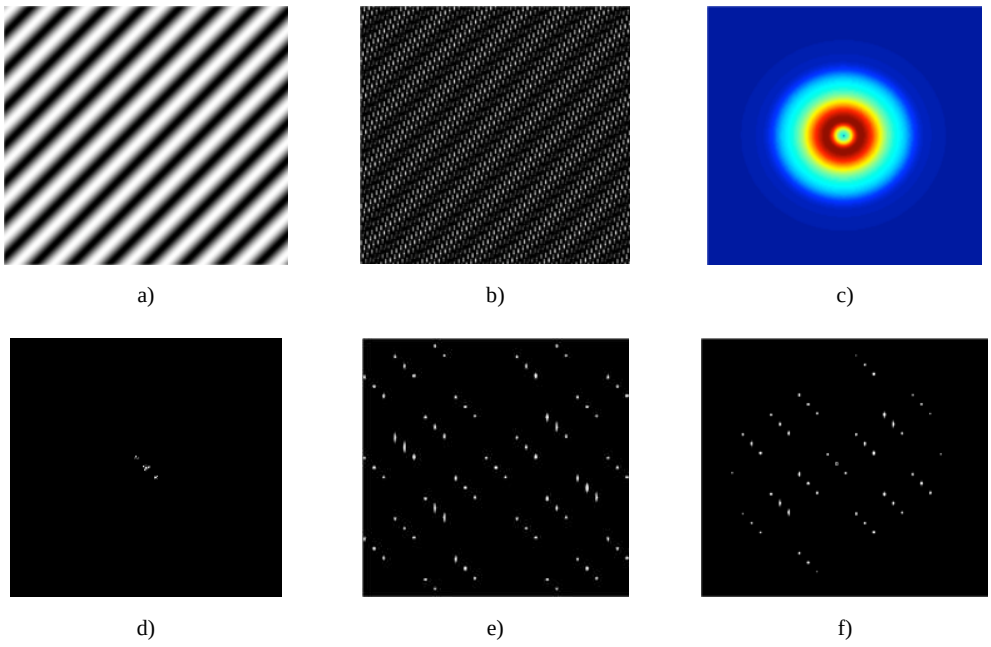

Figure 11. Intermediate stages of the pass/fail analysis: a) input signal, b) output signal, c) CSF weighting window, d) spectrum of the input signal, e) spectrum of the output signal, f) weighted spectrum of the output signal.

Our pass/fail analysis has the following steps. Given a particular input signal we calculate its spectrum (magnitude of the 2D FFT). We find the largest peak in the spectrum of the input signal (disregarding the DC component) and record its amplitude Ref_{val} and position Ref_{pos}. We calculate the spectrum of the output signal, and model the contrast sensitivity

function by applying a circular weighting window. The weights in the window change as a function of the distance to the center of the coordinate system, the shape of the function follows the shape of the spatial CSF at photopic (daylight) level as described in [9], and the scale of the window is calculated for an observation distance of 50cm. After applying CSF weights to the output spectrum, we measure in the same position (Ref_{pos}) and record the amplitude $O1_{val}$. Then, disregarding the DC component and the peak at position Ref_{pos}, we find the biggest of the remaining peaks and record its value $O2_{val}$. If the ratio $O1_{val}/O2_{val}$ is higher than 4 (e.g. $O2_{val}$ is less than 25% of $O1_{val}$) we deem the input frequency to belong to passband. As an example, the data in various stages of such test can be seen in Figure 11. An input signal under test is shown in Figure 11a, and its frequency spectrum is given in Figure 11d. The output signal simulated for a multi-view display is shown in Figure 11b, and its frequency spectrum – in Figure 11e. The CSF weighting coefficients for observation distance of 50cm are shown in Figure 11c, and the weighted spectrum of the output signal is given in Figure 11f.

4.3 Passband estimation framework

In order to obtain the full 3D passband of a display, one would need to test input signals containing all combinations of spatial and angular frequencies. In our experiments, we used a set of test signals with varying horizontal, vertical and angular frequency. Each test signal is a 3D volume in (x, y, o) space, and the intensity of each point in the volume is described by

$$I_{x,y,o} = \frac{1}{2}\sin(\pi \cdot x \cdot f_x + \pi \cdot y \cdot f_y + \pi \cdot o \cdot f_o) + \frac{1}{2} \quad (1)$$

where f_x, f_y are expressing the number of cycles per centimeters across the display surface in x and y direction, and $f_o$expresses the number of cycles per centimeter along the observation line.

We created a passband estimation framework and used it to derive the 3D passbands of the "multi-view" and the "light-field" display models described earlier. The framework has the following stages, as shown in Figure 12. We select a triplet of f_x, f_y, f_o frequencies. Using these frequency values, a test signal is being rendered. The rendering is done two times – once simulating the output of the display under test, and once directly with the full output resolution. The output resolution is chosen to be sufficiently higher (10 times) than the highest frequency under test. The simulation of the display output has three steps – first the test signal is sampled in the position of rays in the display model, then the angular visibility and ray point-spread functions are applied, and finally the image is rendered with the output resolution. These steps simulate the ray generation, LF reconstruction of the image, and capturing the output respectively. The direct rendering branch is sampling the test signal with the full output resolution. The simulation branch simulates the display image for particular observation angle, while the direct rendering branch produces the reference output for the same observation angle. The display output is compared to the reference output in a pass/fail test. This comparison is done for a number of positions on the observation line, with a step of 2mm. We have selected 3mm step as being the typical size of the pupil of the human eye [10]. If the pass/fail test has a positive result for all observation positions inside the display field-of-view, the f_x, f_y, f_o frequency triplet is deemed to belong to the 3D passband of the display – i.e. for that triplet the dominant frequency is preserved for all observation positions. The 3D passband is built by testing different f_x, f_y, f_o combinations. In our experiments, we scanned the range $f_x \in [-5; 5], f_y \in [-5; 5], f_o \in [-1;1]$.

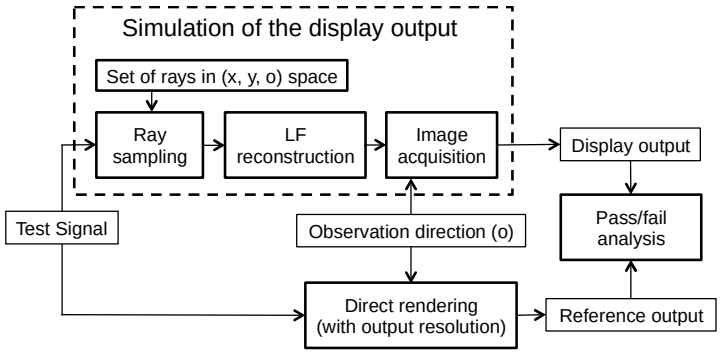

Figure 12. Passband estimation framework

5. RESULTS

We used the passband estimation framework to derive the 3D passbands of the multi-view and the light-field display models. Both models use approximately the same amount of rays (0.02% difference) but they differ in the way the rays are distributed along the observation line. The multi-view display model has 8 groups of rays, where all rays inside one group cross the observation line at the same spot (i.e. the optimal observation position of the view). The light-field display model has its rays randomly distributed along the observation line. The estimated passbands of both models are substantially different, as it can be seen in Figure 13.

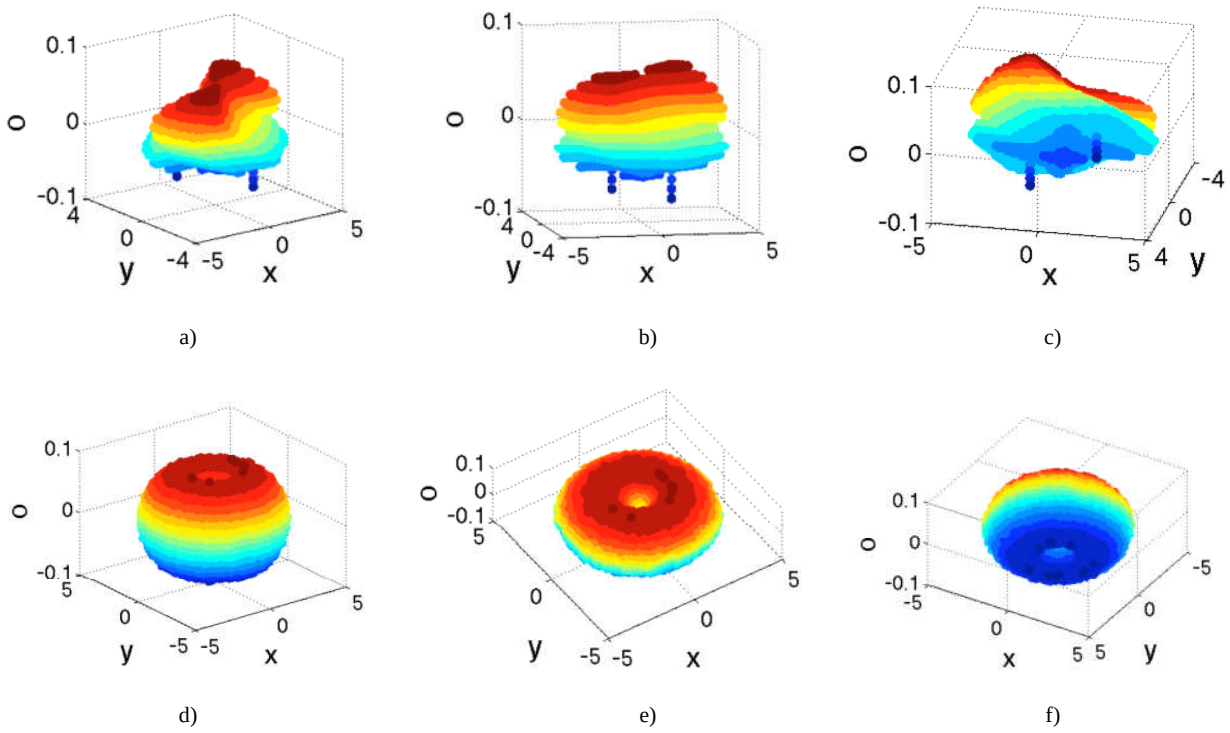

Figure 13. Derived 3D passbands: a)-c) Simulated passband of multi-view display, d)-f) Simulated passband of light-field display

The multi-view display passband (Figure 13abc) has an asymmetric shape. In the x/y plane (representing spatial resolution) the passband has an anti-symmetric shape - image details with certain orientation are more "favorably" represented. This effect matches our previous observations that the display is better at representing slanted lines with orientation matching the one of the parallax barrier (see Figure 2a) [5]. There is also asymmetry along (o) direction of the passband – for example lines with positive slant and positive parallax pass through with fewer distortions than the same lines with negative parallax. This is an effect of the parallax barrier. The sub-pixels which belong to two neighboring view appear on identical, but shifted grids[5]. For an observer moving along the observation line the grid of visible sub-pixels exhibits slight apparent shift (see Figure 9b). Input signals with certain parallax values are a better "match" to the apparent shift of the parallax barrier –thus they are represented with fewer distortions.

The light-field passband (Figure 13def) has symmetric and compact appearance. It has a toroid shape - low spatial frequencies with high angular component exhibit higher level of distortions than medium spatial frequencies with the same angular component. The reason for that is the CSF of the vision. Due to rays appearing on a non-rectangular grid, the introduced by the light-field display appear as wide-spectrum noise (see Figure 10c). Given two signals with the same amplitude, and a constant level of distortions, a signal with medium frequency would be more visible than another one with very high or very low frequency – thus, signals with frequency of 1 to 3 cycles per degree are more "robust" to distortions. The comparison between the passbands is summarized in Table 1. The passband of the light-field model has

more uniform and compact shape, and the number of points belonging to the passband is 2.2 times higher compared with the passband of the multi-view display.

Table 1 – Comparison between the simulated 3D passbands of multi-view and light-field displays

	x range	y range	o range	Passing points	Distribution
Multi-view model	-4.1..+4.1	-2.8..+2.8	-0.06..+0.06	5904	Non-uniform
Light-field model	-3.6..+3.6	-3.6..+3.6	-0.08..+0.08	13253	Uniform

6. CONCLUSIONS

We have presented a methodology for deriving the so-called *3D passband* of any 3D display that provides horizontal head parallax. We proposed to represent the output of such displays as a set of rays in a specific (x, y, o) coordinate. We created a simulation framework, which can use the ray-set models to render the expected output of such display for a given observation position. We proposed an analysis algorithm, which can assess the perceptual effect of the distortions introduced by a light-field 3D display. We use the simulation framework to "scan" a large set of test signals and derive the passband of the display model.

We created two display models – one to represent a typical multi-view display, and another to represent a typical projection-based light-field display. We have derived their passbands. The results suggest, that within a given budget of rays, the ray distribution of a typical light-field display results on a better bigger passband and a better ability to represent diverse 3D content.

ACKNOWLEDGEMENT

This work is supported by the PROLIGHT-IAPP Marie Curie Action of the People programme of the European Union's Seventh Framework Programme, REA grant agreement 32449.

REFERENCES

1 S. Pastoor, "3D displays," in *3D video Communication*, O. Scheer, P. Kauff and T. Sikora, Eds., Chichester, West Sussex, Wiley, 2005, pp. 235-260.

2 W. IJsselsteijn, P. Seuntiens and L. Meesters, "Human factors of 3D displays", in (Schreer, Kauff, Sikora, edts.) *3D Video Communication*, Wiley, 2005.

3 N. Dodgson, "Autostereoscopic 3D Displays," *Computer*, vol.38, no.8, pp. 31- 36, Aug. 2005, IEEE, 2005.

4 T. Balogh, "The HoloVizio system," Proc. *SPIE 6055, Stereoscopic Displays and Virtual Reality Systems XIII*, 60550U (January 27, 2006); doi:10.1117/12.650907

5 A. Boev, R. Bregovic and A. Gotchev, "Measuring and modeling per-element angular visibilty in multiview displays," *Special issue on 3D displays, Journal of Society for Information Display*, vol. 18, no. 9, pp. 686-697, Sept. 2010.

6 B. A. Wandel, Foundations of vision, Sunderland, Massachusetts, USA: Sinauer Associates, Inc, 1995.

7 D. Chandler, "Visual Perception - Introductory Notes for Media Theory Students," MSC portal site, University of Wales, Aberystwyth, 2008. [Online]. Available: http://www.aber.ac.uk/media/sections/image.html.

8 A. Boev, R. Bregovic and A. Gotchev, "Visual-quality evaluation methodology for multiview displays," *Displays*, vol. 33, no. 2, pp. 103-112, April 2012.

9 Maria Amparo Díez-Ajenjo, Pascual Capilla, Spatio-temporal Contrast Sensitivity in the Cardinal Directions of the Colour Space. A Review, Journal of Optometry, Volume 3, Issue 1, 2010, Pages 2-19, ISSN 1888-4296, 10.3921/joptom.2010.2.

10 M. W. Halle, "Holographic stereograms as discrete imaging systems," in Practical HolographyVIII, SanJose, CA.